

Discerning In-Situ Performance of an Enhanced-Oil-Recovery Agent in the Midst of Geological Uncertainty: II. Fluvial-Deposit Reservoir

S. A. Fatemi, J.-D. Jansen, and W. R. Rossen, Delft University of Technology

Summary

An enhanced-oil-recovery (EOR) pilot test has multiple goals, among them to be profitable (if possible), demonstrate oil recovery, verify the properties of the EOR agent in situ, and provide the information needed for scaleup to an economical process. Given the complexity of EOR processes and the inherent uncertainty in the reservoir description, it is a challenge to discern the properties of the EOR agent in situ in the midst of geological uncertainty. We propose a numerical case study to illustrate this challenge: a polymer EOR process designed for a 3D fluvial-deposit water/oil reservoir. The polymer is designed to have a viscosity of 20 cp in situ. We start with 100 realizations of the 3D reservoir to reflect the range of possible geological structures honoring the statistics of the initial geological uncertainties. For a population of reservoirs representing reduced geological uncertainty after 5 years of waterflooding, we select three groups of 10 realizations out of the initial 100, with similar water-breakthrough dates at the four production wells. We then simulate 5 years of polymer injection. We allow that the polymer process might fail in situ and viscosity could be 30% of that intended. We test whether the signals of this difference at injection and production wells would be statistically significant in the midst of geological uncertainty. Specifically, we compare the deviation caused by loss of polymer viscosity with the scatter caused by the geological uncertainty using a 95% confidence interval. Among the signals considered, polymer-breakthrough time, minimum oil cut, and rate of rise in injection pressure with polymer injection provide the most-reliable indications of whether a polymer viscosity was maintained in situ.

Introduction

Chemical-EOR processes represent a small fraction of commercially successful EOR projects. This is in part because of uncertainty in predictions of process performance (Sheng 2011; Lake et al. 2014). For polymer flooding, the integrity of in-situ polymer viscosity is essential for the effectiveness of the process, and its behavior can be uncertain (Weiss and Baldwin 1985). It is important to determine whether an EOR process achieves its design properties in situ because a process that did not achieve the desired objectives in one formation might be successful in another field if it demonstrates that it achieves its technical objectives. A key problem in discerning process performance is distinguishing it in the midst of geological uncertainty. Was an unexpected result caused by the injectant failing to achieve its design properties in situ, or because of unexpected geology?

Researchers have studied uncertainty in EOR-process performance and uncertainty in the geological description, but not the two together. Previous research has examined uncertainty in performance parameters of surfactant flooding (interfacial tension) and carbon dioxide EOR (asphaltene deposition or minimum miscibility pressure) (Brown and Smith 1984; Denney 2011; Stanley 2014). There have also been studies of the effect of geological heterogeneities and their uncertainty on how an EOR process performs. Heterogeneity and geological factors have different effects on the various EOR processes, including polymer and alkaline/surfactant/polymer and thermal and gas-injection (miscible and immiscible) EOR. Studies of the effects of geological heterogeneity and uncertainty on EOR performance include Chen et al. (2008), Kumar et al. (2008), Popov et al. (2010), and Soleimani et al. (2011).

Interpretation of field-pilot results requires the ability to distinguish the effects of geological and process-performance uncertainty. Unexpected results could arise from a misunderstanding of either the geology of the reservoir or the EOR process. In this paper, we investigate the effect of both sources of uncertainty together in a statistical approach using the work flow described in Fatemi et al. (2017). The work flow displays the key steps of discerning in-situ performance of an EOR process in the midst of geological uncertainty in an organized structure in which two sources of uncertainty are defined: uncertainty in the performance of the EOR process itself and uncertainty in our knowledge of the subsurface. Briefly, the work flow begins with an ensemble of reservoirs representing the range of reservoir descriptions consistent with the geological data and production performance to date, and a listing of key possible mechanisms of process failure in situ. For each mechanism, a set of simulation parameters representing the design process and a set representing failure by the given mechanism are identified. A set of “signals,” or characteristics of production behavior (such as injection-well pressure or cumulative oil recovery), is also identified. The process is simulated on each of the reservoir descriptions in the ensemble, for the set of parameters representing a successful process and for that representing an unsuccessful process. If, for a given signal, the failed process lies outside the statistical confidence interval according to the simulations of a successful process, then that signal can distinguish process failure in the midst of geological uncertainty.

For simplicity, we consider here a polymer process with a single mechanism of failure: polymer fails to achieve its design viscosity in situ. In Fatemi et al. (2017), we used for illustration a layer-cake model with an extreme level of geological uncertainty; here we apply the work flow to a case with a more-realistic geological model and a level of uncertainty that is more representative of a field after a period of waterflood. We present a case study derived from the “modified egg model” (Jansen et al. 2014) to illustrate this challenge: a polymer EOR process designed for a 3D fluvial-deposit water/oil reservoir. The polymer is designed to have a viscosity of 20 cp in situ. We start with 100 realizations of this 3D reservoir to reflect the range of possible geological structures honoring the statistics of the initial geological uncertainties. We next group the realizations according to a measure of similarity that reflects the interaction between heterogeneity and the reservoir-flow mechanisms (Mantilla and Srinivasan 2011). After 5 years of waterflooding, we

rank the reservoir models in different groups of 10 realizations, out of the initial 100 equally probable realizations, with similar water-breakthrough dates at the four production wells. We form three sets of 10-member realizations and apply the methodology accordingly. Each group of 10 realizations thus represents a range of geological uncertainty remaining after 5 years of waterflood.

For a polymer flood to meet its technical success, we want the polymer in-situ viscosity (as one of the more-important properties of the polymer-process design) to meet its technical design value. Then, to represent EOR-process failure, we allow that the polymer process might fail in situ and viscosity could be 30% of that intended. This failure could be the result of mechanical degradation in surface facilities or when entering the perforations, faulty translation from laboratory-measured properties to properties in situ, faulty characterization of resident reservoir brine, or chemical or biological degradation of the polymer. We then simulate 5 years of polymer injection. We assume that throughout the reservoir, polymer viscosity is less than the design value. We test whether the signals of this difference at injection and production wells would be statistically significant in the midst of the geological uncertainty. Specifically, we compare the deviation caused by loss of polymer viscosity with the scatter caused by the geological uncertainty using a 95% confidence interval. Various signals are monitored to see which are the most-reliable indications of whether a polymer viscosity was maintained in situ. We further investigate the statistical significance of each signal.

The work flow presented here could be applied to other EOR processes by defining possible mechanisms of failure for those processes.

Case-Study Description

We consider a modified version of the standard “egg model,” which is a fluvial-deposit water/oil-reservoir model containing eight injection wells and four production wells (Jansen et al. 2014) derived from van Essen et al. (2009). The model has seven layers and contains 18,553 gridblocks, each $8 \times 8 \times 4$ m in size. Production from the reservoir is simulated over a time horizon of 5 years of waterflood followed by 5 years of polymer flood. The average reservoir pressure is set at 400 bar, and the initial water saturation is taken to be uniform over the reservoir at a value of 0.1. More details on the geological and fluid properties used in this case study are presented in **Table 1**. The reservoir is in a fluvial-depositional environment with a known main-flow direction. A set of 100 geological realizations of the reservoir was generated by van Essen et al. (2009), depending on geological insight rather than a geostatistical method. The 100-realizations amount is assumed to be large enough to be a good representation of this range (van Essen et al. 2009). We have modified the oil viscosity in this model to make the reservoir a candidate to undergo polymer flood (Dickson et al. 2010). The well locations and absolute-permeability field of the first realization of the set are depicted in **Fig. 1**. **Fig. 2** displays the absolute-permeability field of six realizations randomly selected from the set, without the wells.

Property	Value	SI Units
Water density	1000	kg/m ³
Oil density	900	kg/m ³
Water viscosity	1	cp
Oil viscosity	20	cp
Water compressibility	10^{-10}	1/bar
Oil compressibility	10^{-10}	1/bar
Initial reservoir pressure	400	bar
Porosity	0.2	—
Endpoint relative permeability, oil	0.8	—
Endpoint relative permeability, water	0.75	—
Corey exponent, oil	4	—
Corey exponent, water	3	—
Residual oil saturation	0.1	—
Connate-water saturation	0.1	—
Capillary pressure	0	Pa
Initial water saturation	0.1	—

Table 1—Reservoir and fluid properties of the modified egg model.

Our case study fits the criteria for a polymer-EOR candidate according to the screening benchmarks suggested by Dickson et al. (2010) and Saleh et al. (2014), as shown in **Table 2**.

Representation of Uncertainty in Polymer Performance. Polymer performance in situ is sensitive to many factors (Lake et al. 2014), including non-Newtonian rheology, permeability reduction, reduction of residual oil saturation, shear degradation, precipitation, adsorption, and chemical and thermal degradation. In principle, each separate mechanism could be considered separately, with simulations of design and failure cases. Our purpose here is not to evaluate a fully mechanistic and predictive model for polymer performance in the field, but to illustrate a method to confirm process effectiveness in situ in the midst of geological uncertainty. Therefore, for simplicity, we assume that polymer simply viscosifies the aqueous phase, with no change in residual oil saturation.

We represent uncertainty in process performance by allowing that polymer viscosity could be 6 or 20 cp in situ. In our simulations, we represent the failure to attain the design viscosity in situ simply by injecting polymer with a concentration corresponding to a viscosity of 6 cp (250 ppm) instead of 20 cp (600 ppm), according to the input-polymer-rheology table in the simulator (Van Doren et al. 2017). Because we exclude adsorption from our study, this change in polymer concentration in the simulation does not retard the advance of the polymer bank. For a different EOR process, the possible mode of failure might be loss of miscibility (miscible flooding) or failure to achieve ultralow interfacial tension (surfactant flooding).

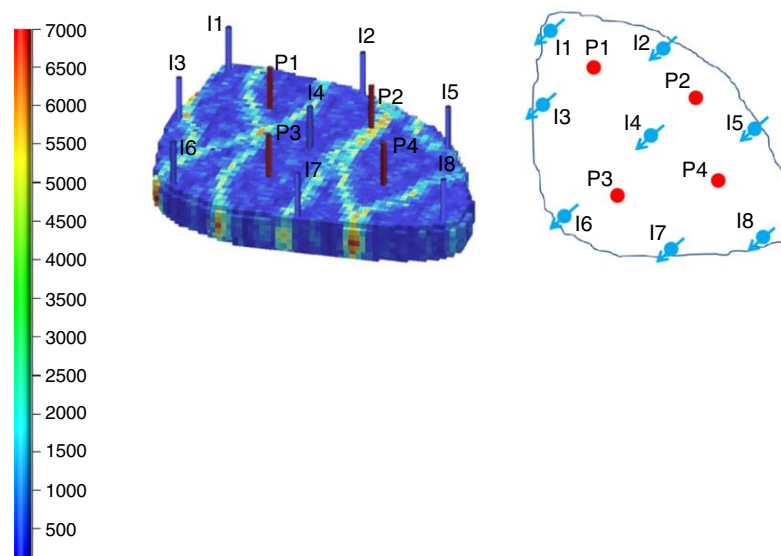


Fig. 1—Permeability field and well locations (Jansen et al. 2014), derived from van Essen et al. (2009).

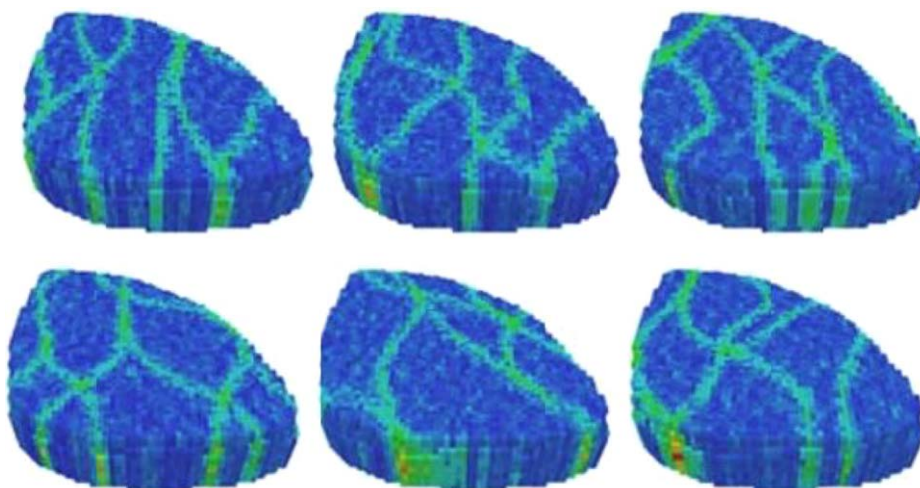


Fig. 2—Permeability field of six randomly chosen realizations out of a set of 100, showing alternative fluvial structures (Jansen et al. 2014), derived from van Essen et al. (2009).

Property	Suggested in Literature	Case Study
In-situ oil viscosity (cp)	10–1,000	20
Average oil saturation at start of polymer flood (%)	>0.30	~0.50*
* Varies among realizations		

Table 2—Suggested values for a reservoir candidate to go through a polymer-flood process, derived from Saleh et al. (2014).

Fractional-Flow Theory in Polymer Flooding. It is useful to perform a 1D fractional-flow analysis of any reservoir system to identify whether it is suitable for a particular recovery process before undertaking a detailed reservoir-simulation study. One of the simplest and most widely used methods of estimating the displacement efficiency in an immiscible displacement process is the Buckley-Leverett method (Craft et al. 1991; Dake 2001; Fanchi 2005; Lake et al. 2014). Our purpose here is to compare the displacement efficiency in one dimension for the design polymer flood with that of the reduced-viscosity polymer flood. The recovery of the 1D polymer flood at polymer breakthrough, mobility ratio at the shock front, and recovery at 2-pore-volume (PV) injection can be extracted from the fractional-flow diagram, as shown in **Table 3**.

Table 3 shows that even in a homogeneous 1D reservoir without gravity segregation, the viscosity reduction results in a lower recovery at polymer breakthrough and after 2-PV injection. In addition, the mobility ratio at the shock front is smaller for the design viscosity than for the reduced viscosity, which suggests better mobility control and a more-uniform sweep in a 3D heterogeneous reservoir for the design-viscosity case.

Representation of Geological Uncertainty. We start with 100 realizations of this reservoir model to reflect the range of possible geological structures reflecting the initial geological uncertainty. Before production begins, all reservoir models are equally probable

because they all honor the static conditioning data and the prior geologic interpretations. After 5 years of waterflood data are collected, however, many of these geological realizations are no longer plausible. To represent the reduced range of possibilities consistent with waterflood data, we choose from the original set groups of reservoirs with relatively similar waterflood performance (specifically, similar waterflood-breakthrough times in the four production wells). Arpat and Caers (2004) introduced the term “distance” between reservoir models, referring to a measure of similarity between different geological-model realizations. We define a parameter to represent the relative difference in water-breakthrough times of the realizations at the four production wells and call it the root-mean-square breakthrough-time difference (RMSBTD) D_{ij} between realizations i and j . It is calculated as

$$D_{ij} = \frac{1}{4} \sqrt{\sum_{k=1}^4 (t_{i,k} - t_{j,k})^2}, \dots \dots \dots (1)$$

where t is the water-breakthrough time and k is a counter over the production wells.

	Design Viscosity, 20 cp	Reduced Viscosity, 6 cp
Oil recovery at polymer breakthrough (%)	47%	40%
Mobility ratio at shock front*	0.26	0.38
Fraction of movable oil recovered at 2-PV injection**	0.97	0.9

* Mobility behind the front divided by mobility ahead of the front.
 ** $(S_{wavg} - S_{wc}) / (1 - S_{wc} - S_{or})$, where S_{wavg} is average water saturation behind the shock front, S_{wc} is connate-water saturation, and S_{or} is residual oil saturation.

Table 3—Recoveries after polymer breakthrough for the design-viscosity case vs. reduced viscosity in 1D secondary polymer flood.

We rank and group realizations according to this parameter. For example, **Fig. 3** shows water production in one of the realizations where water breakthrough occurs early in the simulation, and **Table 4** shows the water-breakthrough time of four production wells for two of the realizations and the accompanying RMSBTD. We build a symmetrical 100×100 matrix of RMSBTD for each realization against all other realizations. From this, we form 10-member cases with similar behavior (i.e., sets with the smallest RMSBTD among all other sets in the matrix). We then rank these 10-member sets in an ascending order according to the RMSBTD value, and further characterize them according to their average water-breakthrough time in each producer.

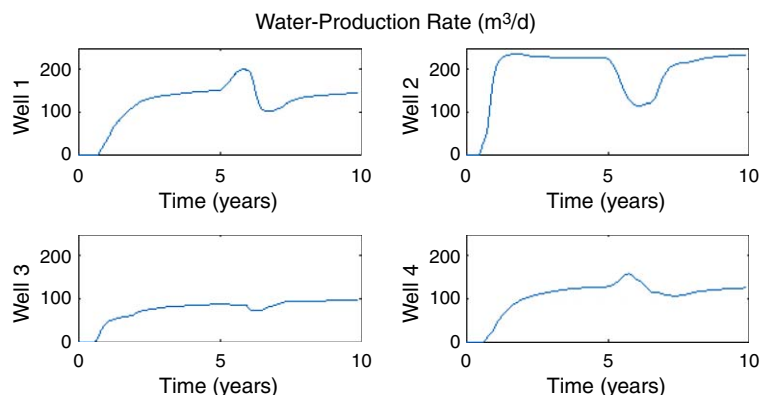


Fig. 3—Water production of four producers in one realization. Water breakthrough occurs early in the simulation.

Realization Number	Producer 1 (days)	Producer 2 (days)	Producer 3 (days)	Producer 4 (days)	RMSBTD (days)
1	285	123	356	341	—
2	510	122	185	442	75

Table 4—Water-breakthrough time of four producers in two different realizations (Realizations 1 and 2) and their typical distance value.

We pick three sets of realizations to represent the reduced geological uncertainty at the start of the polymer flood (i.e., after 5 years of waterflood). The first set has the smallest RMSBTD value (least variability in water-arrival times at all wells) among the three sets: 22 days. The earliest waterflood breakthrough in this set occurs in Producer P2 in almost all its members, with an average of 175 days. There is a high-permeability channel directly to Injectors I2 and I4 in all cases in this set. The members of the second set, with a larger RMSBTD (more-variable water-breakthrough times) of 28 days, do not overlap with members of the first set. The earliest waterflood-breakthrough time occurs mainly in Producer P2 (average time = 177 days). There is a high-permeability channel to Injectors I2, I4, and I5 in most members of this set. An exceptionally slow breakthrough at Producer P1 (474 days) also characterizes this set. The third set, with a somewhat larger RMSBTD of 29 days, has no members in common with the second set, and eight of 10 of its members are distinct from the first set. For most members, waterflood-breakthrough time is earliest in Producer P3 (average time = 185 days). In this

case, there is a high-permeability channel to Injectors I4, I6, and I7. Appendix A provides details of waterflood-breakthrough times of the three sets.

Thus, the three sets represent three cases of roughly similar waterflood behavior within the set but different behavior between sets, in terms of which injectors are linked by the high-permeability channels to which producers. In one set, a producer is relatively unconnected to any injector.

On these three 10-member groups of realizations representing reduced geological uncertainty, we run our polymer-flood simulations and implement our uncertainty-analysis approach.

In a field application, one would use an ensemble of reservoir models consistent with the geological setting, geophysical and log data, and production data during the period of waterflood.

Development Scenario and Procedure

We run the polymer-flood simulations using a proprietary fully implicit reservoir simulator (Van Doren et al. 2011). In each simulation run, 5 years of water injection is followed by 5 years of polymer-slug injection. **Figs. 4 through 6** show results of the simulation for four producers and eight injectors for one of the realizations.

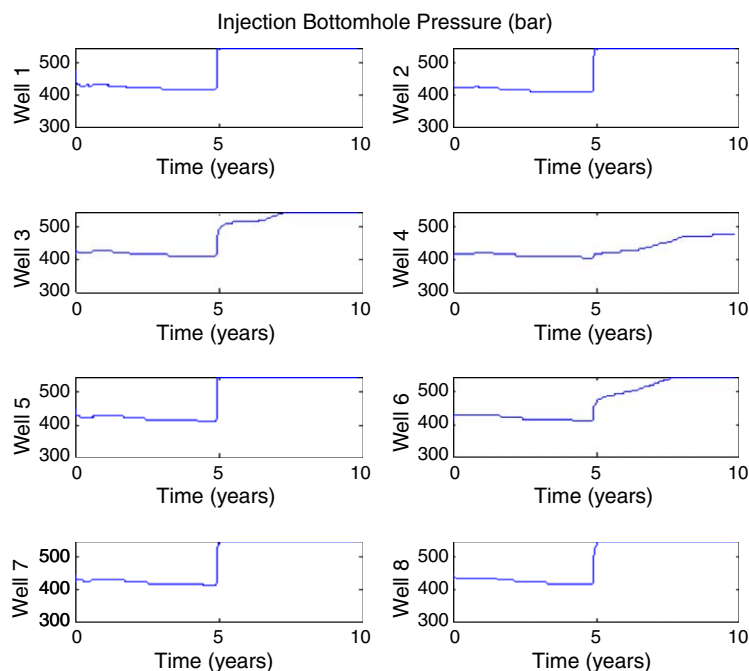


Fig. 4—Injection bottomhole pressure of eight injectors.

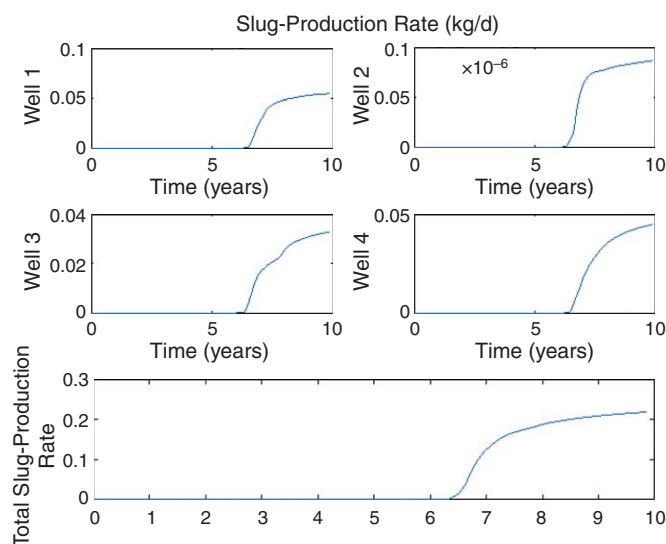


Fig. 5—Polymer-slug-production rate in four producers and total polymer-production rate.

Polymer-injection wells are liable to an unknown extent of fracturing during polymer injection (Seright et al. 2009). Rather than represent this fracturing and the increase in injectivity explicitly, we represent the resulting increased ability to inject polymer indirectly

by allowing a very large maximum value of injection-well pressure (545 bar) during polymer injection. This is not the actual injection pressure of these wells, but allows indirectly for increased polymer injection in these wells without representing the fracturing process explicitly.

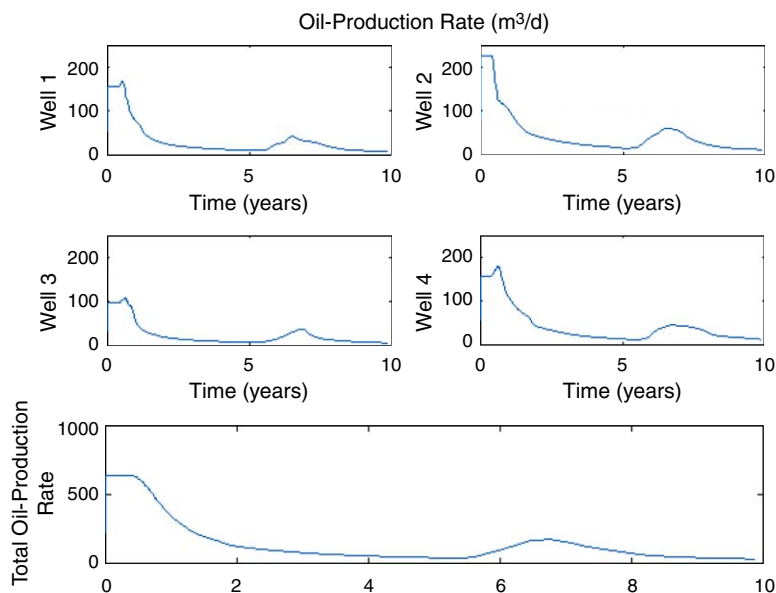


Fig. 6—Oil-production rate in the four producers and total oil-production rate.

As shown in Fig. 3, water is injected for 5 years, and it breaks through early in the waterflood phase in the four production wells. A polymer slug is then injected and causes a rise in injection pressure, as shown in Fig. 4. Breakthrough of polymer occurs sometime after injection, as illustrated in Fig. 5. Fig. 6 shows the oil-production profile in four producers for one realization; there is incremental oil produced because of the polymer flood. We identify the five polymer-flood signals to study (Fatemi et al. 2017) as

1. Polymer-breakthrough time (in years) (“polymer BT”)
2. Change in injection pressure upon polymer injection in 1 year (in bar) (“rise in P_{inj} ”)
3. Minimum oil cut (“min. oil cut”)
4. Time of initial increase in oil-production rate (in years) (“oil-bank arrival time”)
5. Cumulative oil production at end of process (in m^3) (“end cumoil”)

Vertical and Areal Sweep

Fig. 7 shows the permeability map of the first realization in the egg model, where we can visually perceive the high-permeability streaks. To analyze the effectiveness of the polymer injection in sweeping the nonchannel pay, we can compare the snapshots of three different times during the simulation run.

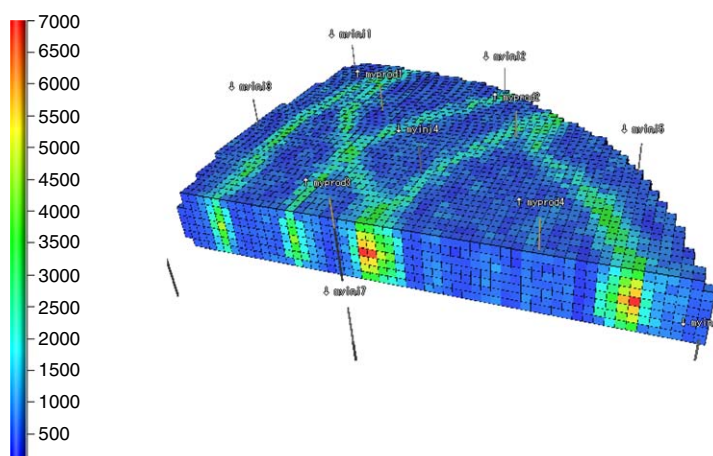


Fig. 7—Slice of the permeability map of Layer 4 of Realization 1.

Fig. 8 shows the oil-saturation map of the reservoir at three different times: around the water-breakthrough time, the end of the waterflood period, and the end of the polymer-flood period for both the 20- and 6-cp in-situ viscosities. As Fig. 8 shows, the polymer flood causes better sweep in the channel pay as well as the nonchannel pay. The less-viscous polymer slug gives worse sweep, especially of nonchannel pay, as shown in Figs. 8c and 8d.

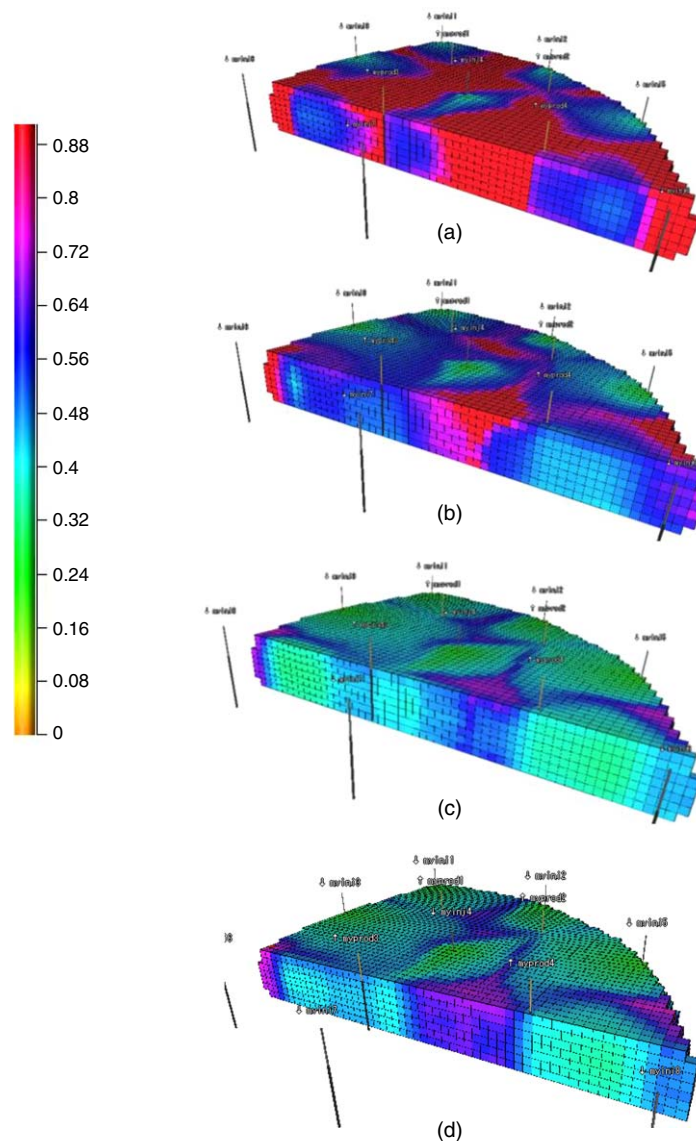


Fig. 8—Oil saturation in Realization 1 at (a) water-breakthrough time; (b) end of waterflood period; (c) end of polymer flood for 20-cp case; (d) end of polymer flood for 6-cp case.

Results

Comparing the signals discussed previously for in-situ polymer viscosity of 20 cp with those for a viscosity of 6 cp, we test whether the signals of this difference at injection and production wells are statistically significant at a 95% confidence level in the midst of geological uncertainty, represented by the 10-member cluster of reservoir descriptions. More specifically, “polymer BT” and “oil-bank arrival time,” which are derived from the first (earliest) producers (of polymer and increased oil cut, respectively) of the four for the 6-cp simulation run, are compared with the population of values for the first producer of the 20-cp-viscosity case. For the rest of the signals, the average values of the four producers (as in “min. oil cut” and “end cumoil”) or eight injectors (as in “rise in P_{inj} ”) are compared with the average signal values of the 20-cp-viscosity representation. As discussed previously, we consider three different sets of realizations. For each reservoir description, we then ask if the given signal with 6-cp polymer viscosity lies in the rejection zone of the confidence interval for the 20-cp-viscosity cases. If the answer is yes, it is labeled as an “outlier” in the adjacent column (meaning the signal can be distinguished in the midst of geological uncertainty), or otherwise labeled as “not outlier” and left as blank in the adjacent column (meaning the signal cannot be distinguished from geological uncertainty). **Table 5** shows the summary of the signal analysis for the case with in-situ 20-cp viscosity for all the production and injections wells of the first set [representing the least RMSBTD (i.e., the set with members most similar to each other)] against the 6-cp case for the first set of realizations. Readers can refer to Appendix B for detailed statistical calculations of the signals for each case.

Of the signals considered, there is one column with only outliers. For this set of realizations, one could discern the effect of viscosity with confidence depending on the “rise in P_{inj} upon polymer injection in 1 year.” This signal could discern the failure of the polymer in situ in the midst of geological uncertainty. If unintended and uncontrolled, fracturing of the injection well is considered likely during polymer injection; however, injection pressure might be a reliable indicator of in-situ polymer viscosity if determined from a diagnostic fracture-injection/falloff test (Craig and Jackson 2017). The signals “polymer breakthrough time” and “time of initial increase in oil-production rate” also discern the effect of viscosity with confidence in almost all the cases. A combination of “minimum oil cut” and “cumulative oil production at end of simulation” could enable one to tell the difference in all the cases.

Tables 6 and 7 show the summarized results for the second and third 10-member sets of geological realizations. We perform the same statistical analysis as described for the first set.

20-cp Global Viscosity vs. 6-cp Global Viscosity for the First Set

Confidence Interval	Rise in P_{inj} , 1 Year	First Polymer-Breakthrough Time (years)	First Oil-Bank Arrival Time (years)	Average Minimum Oil Cut	End Cumulative Oil (m^3)
Upper limit	0.3312	6.47	5.30	0.083	564
Lower limit	0.2232	5.25	4.84	0.053	514
Outliers detected (out of 10)	10	8	9	5	6

Table 5—Summary of the results of discerning the process with 6-cp polymer viscosity from the case with 20-cp polymer viscosity for the first 10-member set of geological realizations.

20-cp Global Viscosity vs. 6-cp Global Viscosity for the Second Set

Confidence Interval	Rise in P_{inj} , 1 Year	First Polymer-Breakthrough Time (years)	First Oil-Bank Arrival Time (years)	Average Minimum Oil Cut	End Cumulative Oil (m^3)
Upper limit	0.352	6.39	5.48	0.089	552
Lower limit	0.195	5.26	4.69	0.050	518
Outliers detected (out of 10)	10	8	7	3	8

Table 6—Summary of the results of discerning the process with 6-cp polymer viscosity from the case with 20-cp polymer viscosity for the second 10-member set of geological realizations.

20-cp Global Viscosity vs. 6-cp Global Viscosity for the Third Set

Confidence Interval	Rise in P_{inj} , 1 Year	First Polymer-Breakthrough Time (years)	First Oil-Bank Arrival Time (years)	Average Minimum Oil Cut	End Cumulative Oil (m^3)
Upper limit	0.331	6.47	5.3	0.083	564
Lower limit	0.223	5.25	4.84	0.053	514
Outliers detected (out of 10)	9	10	6	6	8

Table 7—Summary of the results of discerning the process with 6-cp polymer viscosity from the case with 20-cp polymer viscosity for the third 10-member set of geological realizations.

In these sets, as in the first set, “rate of rise in P_{inj} ” and “polymer-breakthrough time” could discern the failure of the polymer in situ in the midst of geological uncertainty in almost all the cases. In addition, combining the signals of “time of initial increase in oil production rate,” “minimum oil cut,” and “cumulative oil production at end of simulation” could enable one to tell the difference in all the cases. In all cases, outlier status was indicated in at least three of the five signals. Specifically, a combination of “minimum oil cut” and “cumulative oil production at end of simulation” identified the outliers in all cases.

Conclusions

We present the modified “egg model” as a case study illustrating the challenges in discerning the properties of an EOR agent in situ from well data in the midst of geological uncertainty. This study extends our earlier work (Fatemi et al. 2017) by including a more-realistic geological description of a more-complex reservoir with multiple injection and production wells. In this case study, gravity affects waterflood sweep but does not dominate it, whereas polymer improves both vertical sweep and the sweep of the lower-permeability regions between high-permeability channels (Fig. 8).

In this case study, signals are more responsive than in Fatemi et al. (2017), mainly because of a more-realistic description of geological uncertainty after a period of waterflooding. The results of this study mostly support the conclusions of Fatemi et al. (2017). Changes in polymer-breakthrough time are again a reliable indicator of failure of in-situ polymer viscosity in this case study. The rate of rise of injection-well pressure during polymer injection is also a reliable indicator, although a diagnostic fracture-injection/falloff test might be necessary to verify reliability of the injection-pressure data (Craig and Jackson 2017). Moreover, in this case study, other signals such as a combination of “time of initial increase in oil production rate,” “minimum oil cut before the oil bank,” and “final cumulative oil recovery” give a statistically significant indication of loss of in-situ polymer viscosity in the majority of the cases. The results are consistent among the three sets of reservoirs with different degrees of similarity within the set; between sets, the different producers either connected directly to specific injectors or were relatively isolated from all injectors.

Extensions to this approach could include direct history matching of the ensemble of reservoirs to a particular set of waterflood data, and inclusion of multiple separate possible mechanisms of EOR-process failure.

Nomenclature

- D = RMSBTD between two geological realizations, days
- k = permeability, m^2
- n = number of samples taken from the population
- P = pressure, bar

S_{or} = residual oil saturation
 S_{wavg} = average water saturation behind the shock front
 S_{wc} = connate-water saturation
 μ_o = viscosity of oil, cp

Subscript

inj = injection

Acknowledgments

This research was performed within the context of the Recovery Factory Program, a joint project of Shell Global Solutions International and Delft University of Technology.

References

- Arpat, G. B. and Caers, J. 2004. A Multiple-Scale, Pattern-Based Approach to Sequential Simulation. In *Geostatistics Banff 2004*, Quantitative Geology and Geostatistics series, Vol. 14, ed. O. Leuangthong and C. V. Deutsch, 255–264. Dordrecht, The Netherlands: Springer.
- Brown, C. E. and Smith, P. J. 1984. The Evaluation of Uncertainty in Surfactant EOR Performance Prediction. Presented at the SPE Annual Technical Conference and Exhibition, Houston, 16–19 September. SPE-13237-MS. <https://doi.org/10.2118/13237-MS>.
- Chen, Q., Gerritsen, M. G., and Kovscek, A. R. 2008. Effects of Reservoir Heterogeneities on the Steam-Assisted Gravity-Drainage Process. *SPE Res Eval & Eng* **11** (5): 921–932. SPE-109873-PA. <https://doi.org/10.2118/109873-PA>.
- Craft, B. C., Hawkins, M., and Terry, R. E. 1991. *Applied Petroleum Reservoir Engineering*, second edition. Upper Saddle River, New Jersey: Prentice Hall.
- Craig, D. P. and Jackson, R. A. 2017. Calculating the Volume of Reservoir Investigated During a Fracture-Injection/Falloff Test DFIT. Presented at the SPE Hydraulic Fracturing Technology Conference and Exhibition, The Woodlands, Texas, 24–26 January. SPE-184820-MS. <https://doi.org/10.2118/184820-MS>.
- Dake, L. P. 2001. *Practice of Reservoir Engineering*, first edition. Developments in Petroleum Science, Vol. 36. New York City: Elsevier Science.
- Denney, D. 2011. Uncertainty Management in a Major CO₂ EOR Project. *J Pet Technol* **63** (7): 112–113. SPE-0711-0112-JPT. <https://doi.org/10.2118/0711-0112-JPT>.
- Dickson, J. L., Leahy-Dios, A., and Wylie, P. L. 2010. Development of Improved Hydrocarbon Recovery Screening Methodologies. Presented at the SPE Improved Oil Recovery Symposium, Tulsa, 24–28 April. SPE-129768-MS. <https://doi.org/10.2118/129768-MS>.
- Fanchi, J. R. 2005. *Principles of Applied Reservoir Simulation*, third edition. Burlington, Massachusetts: Elsevier.
- Fatemi, S. A., Jansen, J. D., and Rossen, W. R. 2017. Discerning In-Situ Performance of an EOR Agent in the Midst of Geological Uncertainty I: Layer Cake Reservoir Model. *J. Pet. Sci. Eng.* **158** (September): 56–65. <https://doi.org/10.1016/j.petrol.2017.08.021>.
- Jansen, J. D., Fonseca, R. M., Kahrobaei, S. et al. 2014. The Egg Model—A Geological Ensemble for Reservoir Simulation. *Geosci. Data J.* **1** (2): 192–195. <https://doi.org/10.1002/gdj3.21>.
- Kumar, M., Hoang, V. T., Satik, C. et al. 2008. High-Mobility-Ratio Waterflood Performance Prediction: Challenges and New Insights. *SPE Res Eval & Eng* **11** (1): 186–196. SPE-97671-PA. <https://doi.org/10.2118/97671-PA>.
- Lake, L. W., Johns, R., Rossen, W. R. et al. 2014. *Fundamentals of Enhanced Oil Recovery*. Richardson, Texas: Society of Petroleum Engineers.
- Mantilla, C. A. and Srinivasan, S. 2011. Feedback Control of Polymer Flooding Process Considering Geologic Uncertainty. Presented at the SPE Reservoir Simulation Symposium, The Woodlands, Texas, 21–23 February. SPE-141962-MS. <https://doi.org/10.2118/141962-MS>.
- Popov, Y., Spasennykh, M., Miklashevskiy, D. et al. 2010. Thermal Properties of Formations From Core Analysis: Evolution in Measurement Methods, Equipment, and Experimental Data in Relation to Thermal EOR. Presented at the Canadian Unconventional Resources and International Petroleum Conference, Calgary, 19–21 October. SPE-137639-MS. <https://doi.org/10.2118/137639-MS>.
- Saleh, L. D., Wei, M., and Bai, B. 2014. Data Analysis and Updated Screening Criteria for Polymer Flooding Based on Oilfield Data. *SPE Res Eval & Eng* **17** (1): 15–25. SPE-168220-PA. <https://doi.org/10.2118/168220-PA>.
- Seright, R. S., Seheult, J. M., and Talashek, T. 2009. Injectivity Characteristics of EOR Polymers. *SPE J.* **12** (5): 783–792. SPE-115142-PA. <https://doi.org/10.2118/115142-PA>.
- Sheng, J. 2011. *Modern Chemical Enhanced Oil Recovery: Theory and Practice*. Burlington, Massachusetts: Elsevier.
- Soleimani, A., Penney, R. K., Hegazy, O. et al. 2011. Impact of Fluvial Geological Characteristics on EOR Screening of a Large Heavy Oil Field. Presented at the SPE Enhanced Oil Recovery Conference, Kuala Lumpur, 19–21 July. SPE-143650-MS. <https://doi.org/10.2118/143650-MS>.
- Stanley, B. 2014. Effect of Uncertainty in PVT Properties on CO₂ EOR. Presented at the SPE Nigeria Annual International Conference and Exhibition, Lagos, 5–7 August. SPE-172430-MS. <https://doi.org/10.2118/172430-MS>.
- Van Doren, J., Douma, S. G., Wassing, L. B. M. et al. 2011. Adjoint-Based Optimization of Polymer Flooding. Presented at the SPE Enhanced Oil Recovery Conference, Kuala Lumpur, 19–21 July. SPE-144024-MS. <https://doi.org/10.2118/144024-MS>.
- van Essen, G., Zandvliet, M., Van den Hof, P. et al. 2009. Robust Waterflooding Optimization of Multiple Geological Scenarios. *SPE J.* **14** (1): 202–210. SPE-102913-PA. <https://doi.org/10.2118/102913-PA>.
- Weiss, W. W. and Baldwin, R. W. 1985. Planning and Implementing a Large-Scale Polymer Flood. *J Pet Technol* **37** (4): 720–730. SPE-12637-PA. <https://doi.org/10.2118/12637-PA>.

Appendix A—Waterflood Behavior for Three Sets of Reservoirs





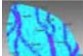





Please see Table A-1.

Number	Realization	Producer 1	Producer 2	Producer 3	Producer 4
1	3	252	151	318	344
2	81	224	139	315	377
3	1	285	123	356	341
4	52	258	184	354	376
5	42	279	185	368	368
6	60	226	142	263	281
7	64	237	213	248	350
8	97	258	159	240	416
9	48	196	247	260	303
10	25	308	202	286	233
—	Average	252.3	174.5	300.8	338.9
Number	Realization	Producer 1	Producer 2	Producer 3	Producer 4
1	51	480	134	209	259
2	86	475	140	156	236
3	40	474	155	155	217
4	47	527	210	187	237
5	63	399	104	246	278
6	20	432	175	251	357
7	31	504	221	286	308
8	67	541	215	144	334
9	39	487	165	363	252
10	18	419	251	294	217
—	Average	473.8	177	229.1	269.5
Number	Realization	Producer 1	Producer 2	Producer 3	Producer 4
1	80	290	292	170	304
2	77	281	253	194	235
3	24	290	359	103	313
4	54	285	313	217	220
5	82	385	321	135	311
6	90	311	193	110	270
7	30	288	408	145	252
8	64	237	213	248	350
9	26	327	379	263	316
10	48	196	247	260	303
—	Average	289	297.8	184.5	287.4

Table A-1—Water-breakthrough time (in days) of the four producers in members of the three selected sets.


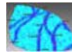





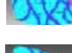


Appendix B

Please see Tables B-1 through B-6.

Realization		Rise in P_{inj} , 5 yr to 6 yr									Polymer Breakthrough (years)				
		Inj 1	Inj 2	Inj 3	Inj 4	Inj 5	Inj 6	Inj 7	Inj 8	Avg	Prod 1	Prod 2	Prod 3	Prod 4	First
	3	0.159	0.105	0.298	0.380	0.380	0.374	0.373	0.373	0.305	6.13	5.65	6.42	6.89	5.65
	81	0.362	0.375	0.282	0.273	0.122	0.363	0.364	0.180	0.290	6.26	5.85	6.38	6.61	5.85
	1	0.166	0.214	0.322	0.388	0.384	0.381	0.242	0.377	0.309	6.23	5.43	6.37	6.87	5.43
	52	0.369	0.368	0.364	0.057	0.126	0.141	0.301	0.363	0.261	6.13	5.87	6.26	6.49	5.87
	42	0.159	0.367	0.304	0.260	0.122	0.194	0.259	0.258	0.240	6.11	6.19	6.36	6.39	6.11
	60	0.354	0.371	0.296	0.049	0.363	0.235	0.362	0.355	0.298	6.14	5.93	6.09	6.75	5.93
	64	0.350	0.349	0.178	0.359	0.154	0.346	0.121	0.355	0.277	6.33	6.45	6.39	6.58	6.33
	97	0.364	0.109	0.263	0.209	0.354	0.278	0.114	0.284	0.247	6.18	5.52	5.86	6.58	5.52
	48	0.348	0.121	0.320	0.348	0.164	0.368	0.296	0.148	0.264	6.04	5.96	5.95	6.44	5.95
	25	0.361	0.369	0.294	0.062	0.365	0.293	0.158	0.336	0.280	6.19	6.27	5.96	6.23	5.96
CI+	—	—	—	—	—	—	—	—	—	0.3312	—	—	—	—	6.47
CI—	—	—	—	—	—	—	—	—	—	0.2232	—	—	—	—	5.25

Oil-Bank Arrival Time (years)					Minimum Oil Cut					End Cumulative Oil $\times 10^3$ (m ³)
Prod 1	Prod 2	Prod 3	Prod 4	First	Prod 1	Prod 2	Prod 3	Prod 4	Average	
5.56	5.70	5.04	5.50	5.04	0.058	0.058	0.061	0.058	0.059	548
5.37	5.14	5.09	5.19	5.09	0.071	0.066	0.066	0.066	0.068	542
5.25	5.56	5.36	5.68	5.25	0.056	0.056	0.056	0.058	0.057	558
5.38	5.08	5.04	5.41	5.04	0.075	0.071	0.072	0.075	0.073	542
5.30	5.22	4.96	5.27	4.96	0.076	0.075	0.075	0.075	0.075	536
5.16	5.13	5.02	5.03	5.02	0.078	0.077	0.075	0.075	0.076	532
5.38	5.08	5.04	5.26	5.04	0.072	0.070	0.070	0.071	0.071	519
5.41	5.75	5.48	5.07	5.07	0.064	0.068	0.064	0.065	0.065	540
5.33	5.50	5.66	5.23	5.23	0.064	0.064	0.066	0.064	0.065	547
5.19	5.30	4.96	5.48	4.96	0.066	0.067	0.068	0.075	0.069	528
—	—	—	—	5.30	—	—	—	—	0.083	564
—	—	—	—	4.84	—	—	—	—	0.053	514

Table B-1—Summary of signal values of the first 10-member set of geological cases calculated for the case with 20-cp polymer viscosity, with upper and lower bounds of the 95% confidence interval (CI+, CI—) for each signal. Inj = injector; Prod = producer.

Realization		Rise in P_{wq} , 5 yr to 6 yr									Polymer Breakthrough (years)						
		Inj 1	Inj 2	Inj 3	Inj 4	Inj 5	Inj 6	Inj 7	Inj 8	Average		Prod 1	Prod 2	Prod 3	Prod 4	First	
	3	0.091	0.052	0.176	0.237	0.231	0.170	0.191	0.214	0.160	Outlier	5.52	5.20	5.84	5.85	5.20	Outlier
	81	0.331	0.306	0.136	0.121	0.075	0.186	0.218	0.110	0.186	Outlier	5.48	5.23	5.59	6.18	5.23	Outlier
	1	0.109	0.237	0.195	0.198	0.260	0.252	0.152	0.287	0.214	Outlier	5.68	5.19	5.64	5.91	5.19	Outlier
	52	0.238	0.316	0.312	0.037	0.070	0.090	0.177	0.179	0.170	Outlier	5.60	5.21	5.67	5.82	5.21	Outlier
	42	0.071	0.329	0.126	0.105	0.070	0.081	0.105	0.104	0.101	Outlier	5.63	5.21	5.69	5.74	5.21	Outlier
	60	0.362	0.255	0.162	0.036	0.204	0.134	0.219	0.254	0.210	Outlier	5.48	5.22	5.55	5.90	5.22	Outlier
	64	0.307	0.309	0.104	0.212	0.092	0.301	0.075	0.304	0.205	Outlier	5.50	5.41	5.79	5.67	5.41	–
	97	0.205	0.015	0.108	0.081	0.313	0.100	0.062	0.117	0.100	Outlier	5.56	5.20	5.52	5.96	5.20	Outlier
	48	0.346	0.364	0.364	0.361	0.288	0.385	0.242	0.128	0.367	Outlier	5.50	5.52	5.40	5.90	5.40	–
	25	0.319	0.331	0.269	0.241	0.354	0.377	0.294	0.389	0.384	Outlier	5.59	5.13	5.58	5.65	5.13	Outlier

Oil-Bank Arrival Time (years)						Minimum Oil Cut						End Cumulative Oil $\times 10^3$ (m ³)	
Prod 1	Prod 2	Prod 3	Prod 4	First		Prod 1	Prod 2	Prod 3	Prod 4	Average			
5.12	5.14	4.39	5.20	4.39	Outlier	0.047	0.047	0.050	0.047	0.047	Outlier	521	—
5.02	4.75	4.67	4.81	4.67	Outlier	0.056	0.051	0.052	0.051	0.053	Outlier	518	—
4.83	5.08	5.19	5.21	4.83	Outlier	0.045	0.044	0.045	0.046	0.045	Outlier	523	—
5.02	4.67	4.38	5.02	4.38	Outlier	0.058	0.056	0.057	0.058	0.057	—	509	Outlier
4.56	4.74	4.28	4.66	4.28	Outlier	0.060	0.060	0.060	0.060	0.060	—	506	Outlier
4.77	4.73	4.45	4.58	4.45	Outlier	0.059	0.059	0.059	0.059	0.059	—	507	Outlier
4.72	4.68	4.64	5.01	4.64	Outlier	0.056	0.056	0.056	0.059	0.057	—	503	Outlier
5.04	5.23	5.06	5.12	5.04	—	0.049	0.050	0.049	0.049	0.050	Outlier	513	Outlier
5.06	5.15	5.24	4.81	4.81	Outlier	0.049	0.049	0.050	0.050	0.050	Outlier	521	—
4.70	4.82	4.45	4.92	4.45	Outlier	0.053	0.054	0.054	0.056	0.054	—	508	Outlier

Table B-2—Discerning the process with 6-cp polymer viscosity from the case with 20-cp polymer viscosity for the first 10-member set of geological realizations. Inj = injector; Prod = producer.

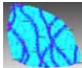
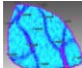
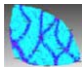
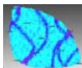
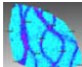
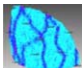
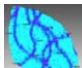
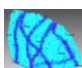
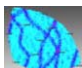
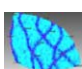
Realization		Rise in P_{inj} , 5 yr to 6 yr	Polymer Break- through (years)	Oil-Bank Arrival Time (years)	Minimum Oil Cut	End Cumulative Oil $\times 10^3$ (m ³)
	51	0.233	5.74	5.00	0.054	524
	86	0.262	5.55	5.03	0.076	534
	40	0.243	5.66	5.14	0.074	537
	47	0.285	6.26	4.99	0.071	542
	63	0.279	5.60	4.96	0.069	534
	20	0.228	5.74	5.08	0.082	551
	31	0.315	6.04	4.95	0.070	534
	67	0.259	5.58	5.02	0.070	533
	39	0.328	5.97	5.08	0.073	532
	18	0.306	6.10	5.55	0.055	528
CI+		0.352	6.39	5.48	0.089	552
CI-		0.195	5.26	4.69	0.050	518

Table B-3—Summary of signal values of the second set of geological realizations with 20-cp polymer viscosity, with upper and lower bounds of the 95% confidence interval (CI+, CI-) for each signal.


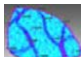








Realization		Rise in P_{inj} , 5 yr to 6 yr		Polymer Breakthrough (years)		Oil-Bank Arrival Time (years)		Minimum Oil Cut		End Cumulative Oil $\times 10^3$ (m ³)	
	51	0.109	Outlier	5.166	Outlier	4.640	Outlier	0.048	Outlier	522	–
	86	0.117	Outlier	5.047	Outlier	4.673	Outlier	0.057	–	510	Outlier
	40	0.123	Outlier	5.031	Outlier	4.719	–	0.056	–	511	Outlier
	47	0.138	Outlier	5.182	Outlier	4.678	Outlier	0.053	–	518	Outlier
	63	0.132	Outlier	4.969	Outlier	4.589	Outlier	0.051	–	513	Outlier
	20	0.109	Outlier	5.161	Outlier	4.709	–	0.059	Outlier	523	–
	31	0.143	Outlier	5.286	–	4.609	Outlier	0.051	–	515	Outlier
	67	0.136	Outlier	4.979	Outlier	4.635	Outlier	0.052	–	510	Outlier
	39	0.145	Outlier	5.203	Outlier	4.589	Outlier	0.052	–	515	Outlier
	18	0.144	Outlier	5.336	–	5.142	–	0.041	Outlier	513	Outlier

Table B-4—Discerning the process with 6-cp polymer viscosity from the case with 20-cp polymer viscosity for the second 10-member set of geological realizations.

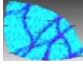
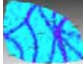
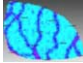

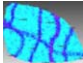
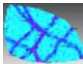
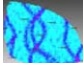


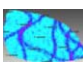
Realization		Rise in P_{inj} , 5 yr to 6 yr	Polymer Break- through (years)	Oil-Bank Arrival Time (years)	Minimum Oil Cut	End Cumulative Oil $\times 10^3$ (m ³)
	80	0.305	5.65	5.04	0.059	548
	77	0.290	5.85	5.09	0.068	543
	24	0.309	5.43	5.25	0.057	558
	54	0.261	5.87	5.04	0.073	542
	82	0.240	6.11	4.96	0.075	536
	90	0.298	5.93	5.02	0.076	532
	30	0.277	6.33	5.04	0.071	519
	64	0.247	5.52	5.07	0.065	540
	26	0.264	5.95	5.23	0.065	547
	48	0.280	5.96	4.96	0.069	528
CI+		0.331	6.47	5.30	0.083	564
CI-		0.223	5.25	4.84	0.053	514

Table B-5—Summary of signal values of the third set of geological realizations with 20-cp polymer viscosity, with upper and lower bounds of the 95% confidence interval (CI+, CI-) for each signal.

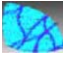
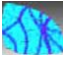








Realization		Rise in P_{inj} , 5 yr to 6 yr		Polymer Breakthrough (years)		Oil-Bank Arrival Time (years)		Minimum Oil Cut		End Cumulative Oil $\times 10^3$ (m ³)	
	80	0.122	Outlier	4.95	Outlier	4.97	–	0.0561	–	512	Outlier
	77	0.151	Outlier	5.14	Outlier	4.78	Outlier	0.0504	Outlier	512	Outlier
	24	0.075	Outlier	4.66	Outlier	4.69	Outlier	0.0527	Outlier	523	–
	54	0.169	–	5.09	Outlier	4.82	–	0.0483	Outlier	517	Outlier
	82	0.102	Outlier	4.74	Outlier	4.96	–	0.0507	Outlier	517	Outlier
	90	0.112	Outlier	4.68	Outlier	4.70	Outlier	0.0635	–	514	Outlier
	30	0.121	Outlier	4.80	Outlier	4.80	Outlier	0.0509	Outlier	518	Outlier
	64	0.165	Outlier	5.06	Outlier	4.80	Outlier	0.0571	–	502	Outlier
	26	0.165	Outlier	5.06	Outlier	4.80	Outlier	0.0571	–	502	Outlier
	48	0.125	Outlier	5.01	Outlier	4.97	–	0.0506	Outlier	522	–

Table B-6—Discerning the process with 6-cp polymer viscosity from the case with 20-cp polymer viscosity for the third 10-member set of geological realizations.

S. Amin Fatemi is a PhD-degree student of petroleum reservoir engineering at Delft University of Technology, The Netherlands. His research interests are reservoir-uncertainty analysis and EOR. Fatemi holds a master's degree in petroleum engineering from Sharif University of Technology, Iran.

Jan-Dirk Jansen is professor of reservoir systems and control and dean of the Faculty of Civil Engineering and Geosciences at Delft University of Technology. He previously worked for Shell International in research and operations. Jansen's current research interests are the development and application of systems and control theory for the management of reservoir flow and induced seismicity. He holds master's and PhD degrees from Delft University of Technology.

William R. Rossen is professor of reservoir engineering in the Department of Geoscience and Engineering at Delft University of Technology. He previously worked at Chevron Oil Field Research Company and was a professor at the University of Texas at Austin. Rossen's current research concerns use of foams for diverting fluid flow in porous media, modeling complex transport processes in networks, and understanding flow in naturally fractured geological formations. He has authored or coauthored more than 90 journal publications. Rossen was named Best Instructor at Delft University of Technology in 2011. He is an SPE Distinguished Member, and in 2012, he was named an IOR Pioneer at the SPE/DOE Symposium on Improved Oil Recovery in Tulsa. Rossen holds bachelor's and PhD degrees from Massachusetts Institute of Technology and the University of Minnesota, respectively, both in chemical engineering.